

The Role of Substrate Curvature in Actin-Based Pushing Forces

Ian M. Schwartz,¹ Morton Ehrenberg,^{1,2}
Michael Bindschadler,^{1,2} and James L. McGrath^{1,*}

¹Department of Biomedical Engineering
University of Rochester
601 Elmwood Avenue
P.O. Box 639
Rochester, New York 14642

Summary

The extension of the plasma membrane during cell crawling or spreading is known to require actin polymerization [1]; however, the question of how pushing forces derive from actin polymerization remains open. A leading theory (herein referred to as elastic propulsion) illustrates how elastic stresses in networks growing on curved surfaces can result in forces that push particles [2, 3]. To date all examples of reconstituted motility have used curved surfaces, raising the possibility that such squeezing forces are essential for actin-based pushing. By contrast, other theories, such as molecular ratchets [4, 5], neither require nor consider surface curvature to explain pushing forces. Here, we critically test the requirement of substrate curvature by reconstituting actin-based motility on polystyrene disks. We find that disks move through extracts in a manner that indicates pushing forces on their flat surfaces and that disks typically move faster than the spheres they are manufactured from. For a subset of actin tails that form on the perimeter of disks, we find no correlation between local surface curvature and tail position. Collectively the data indicate that curvature-dependent mechanisms are not required for actin-based pushing.

Results and Discussion

To critically investigate the requirements of substrate curvature in actin-based motility, we manufactured polystyrene disks and coated them with ActA, the surface protein used by the intracellular pathogen *Listeria monocytogenes* to polymerize host cell actin and become motile [6, 7]. In recent years polystyrene spheres coated with ActA [8], N-WASP [9], or a peptide spanning N-WASP's essential VCA domain [10] have been used to reconstitute motility in extracts and pure proteins. We manufactured disks by pressing 3.4 μm diameter polystyrene spheres between heated glass slides (see Supplemental Data for details on all methods). The resulting particles have flat faces $\sim 5 \mu\text{m}$ in diameter and are $\sim 0.8 \mu\text{m}$ thick (Figure 1). For particles that are aggregated prior to compression so that their lateral expansion is restricted, perimeters emerge with both flat and curved spans (Figure 1). For motility experiments, disks are coated with saturating amounts of ActA and placed in thin (8–12 μm tall) motility chambers containing brain

extracts, an ATP regeneration system, and fluorescently labeled actin for visualization.

In motility chambers, ActA-coated disks were either nonmotile and surrounded by diffuse actin clouds or found in one of several motile configurations (Figure 2A). To explore the temporal relationship between these states, we documented the evolution of the system for 5 hr after the introduction of disks to motility chambers (Table S1). We found that a diffuse cloud of fluorescent actin surrounds all polystyrene disks within 10 min. Over the next few hours, greater than 90% of the particles become motile as clouds transform into tails that push the disks through extracts. Tails may be centered on the perimeters or faces of disks. At all times the most common motile configuration has a tail emanating from each face of a disk, and particles with a tail centered on only one face are the most rare. Eventually, two-thirds of the disks have two face tails. The data suggest that clouds are precursors to both perimeter and face tails and that single face tails may be an unstable configuration (Table S1).

By analyzing particle motion using time-lapse microscopy, we found that disks moving via face tails have higher average speeds than disks moving with perimeter tails or ActA-coated versions of the microspheres used to make disks (Figure 2B). In the common configuration where disks have two face tails, the tails are often positioned to push cooperatively (Figure 2C); however, there are also periods where the opposing tails compete and the particle speed is low (see Movie 1).

To establish that actin polymerization can push against a flat surface, we present selected examples of motility in Figure 3. Choosing particular examples is necessary because while it is possible to infer the net forces acting on a particle from its motion, there are many possible force distributions that can give the same net forces. Also complicating is the fact that because disks are finite in size, curvature-derived forces may act at their edges. Thus the examples shown in Figure 3 are selected because they provide clear examples of pushing against flat faces.

In the first example of Figure 3, a disk is fused to an incompletely compressed particle. The clockwise motion of the assembly suggests that the largest pushing forces occur along the flat face of the disk (Figure 3A; Movie 2). If pushing occurred exclusively on the curved paths of the incompletely compressed particle, the assembly should rotate counterclockwise. The second example shows a disk moving in a spiral due to the constraints of its own tail (Figure 3B; Movie 3). Fluorescent actin contacts the disk on one flat face but also advances around the disk's left periphery. Because the disk advances as it turns, pushing likely occurs on the face and on the periphery, but only pushing forces on the face can explain the counterclockwise rotation of the disk. The third case shows the motion of a pair of contacting disks each with tails centered on one flat face (Figure 3C; Movie 4). In general the assembly rotates and translates (see Movie 4), but during the two intervals shown the assembly moves in a direction normal to the

*Correspondence: jmcgrath@bme.rochester.edu

²These authors contributed equally to this work.

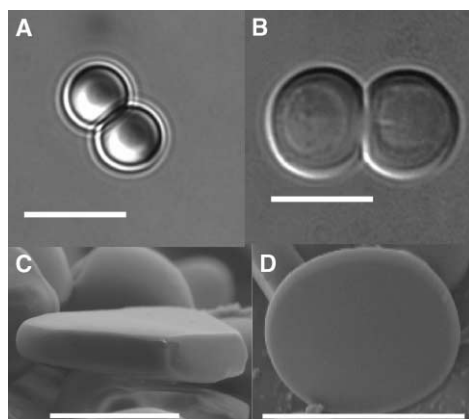


Figure 1. Making Polystyrene Disks

(A) Light microscope image of a particle doublet before compression. A solution of polystyrene microspheres ($3.4 \mu\text{m}$) was dried on clean glass slides so that small aggregates were common. (B) Image of a doublet after compression. Compression of the spheres under heat produces flat faces but perimeters of mixed curvatures because lateral expansion is restricted between particle contacts. (C and D) Scanning electron micrographs of particles. The particle in (C) emerged from an aggregate while that in (D) was isolated during compression. All scale bars represent $5 \mu\text{m}$.

face of one of the disks, most consistent with pushing on that face. During the first of these intervals (Figure 3C, top row), a bright spot in upper tail moves backward in the image despite the forward motion of the assembly. This suggests that this tail is not sufficiently anchored to the environment to help push and further argues that the assembly is pushed by the lower tail in a direction normal to disk face it contacts.

A final example, provided as Supplemental Data (Figure S1; Movie 5), shows a clockwise rotation of a disk that suggests pushing along the flat portions of its perimeter. This occurs despite the fact that actin contacts both flat and curved spans of the perimeter. If pushing were confined to curved spans of the perimeter, the disk would rotate counterclockwise instead. A periodic pattern of fluorescence, described elsewhere as “hopping” [9] is apparent in Figure S1. Hopping was occasionally seen when particles moved with tails on their perimeters (Figure S1; Movies 5 and 6) but never observed for disks moving via face tails.

To investigate a possible relationship between surface curvature and tail positioning, we examined the subset of disks moving with tails on perimeters with both flat and curved spans (typically $\sim 20\%$ of the span of these perimeters was contiguous flat; see Figure 1B). By measuring fluorescence emanating from the digitized perimeters of disks (Figure 4A), we first established that curvature did not bias actin nucleation during cloud formation (Figure 4B). A similar digitization allowed us to correlate the location of tails with local curvature. After normalizing the histogram of tail appearances with respect to the amount of perimeter associated with each of three classes of curvature (convex, flat, or concave), we found no statistical difference between the numbers of tail appearances on flat versus curved perimeters (Figure 4C). Thus the most reasonable interpretation of our data is that tails appear randomly on disk perimeters

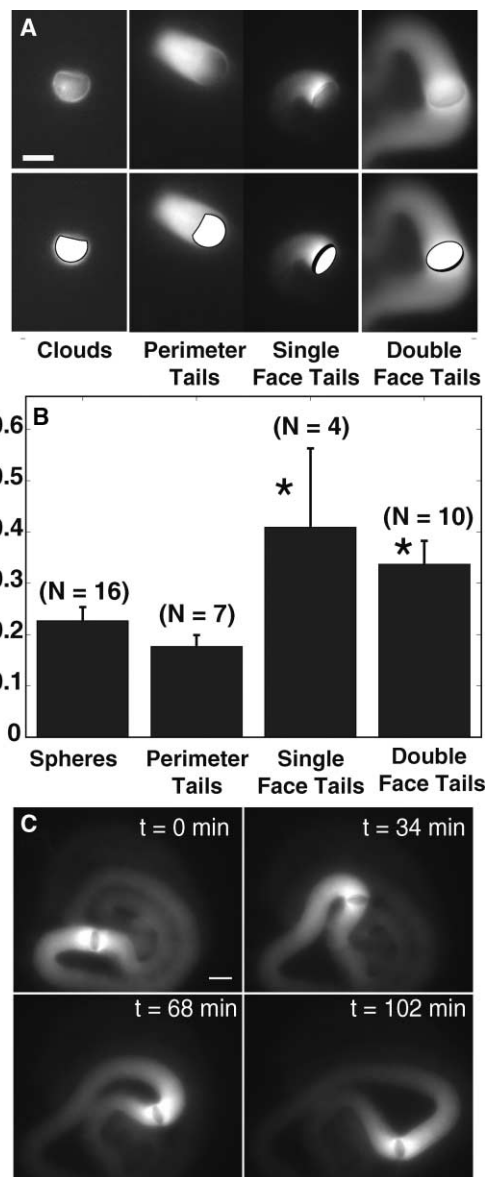


Figure 2. Disk Behaviors in Motility Media

(A) Disk classifications. Disks could be classified as having: clouds (nonmotile nucleation stage), perimeter tails, single-face tails or double-face tails. Disks were added to motility media containing fluorescent actin for visualization. Our interpretations of disk positions are drawn in the second row. The time course of experiments was studied (Table S1); after an initial nucleation phase of ~ 1 hr, the most common configuration was a double-face tail. (B) Disk velocities. The velocity of disks was measured in time-lapse movies by computing the motion of centroids of digitized disk outlines. Error bars are standard errors of the mean and stars indicate significance compared to uncompressed $3.4 \mu\text{m}$ microspheres (ANOVA, $p < 0.05$). (C) Motion of a double-face tail configuration. Mean speed is $\sim 0.37 \mu\text{m}/\text{min}$. Times are relative to initial frame. The scale bar represents $5 \mu\text{m}$. Frames are from Movie 1.

and that factors other than curvature explain the positioning of tails on disks.

Our data on the behaviors of ActA-coated disks are most significant given a leading theory (elastic propulsion) suggesting curvature-dependent mechanisms for

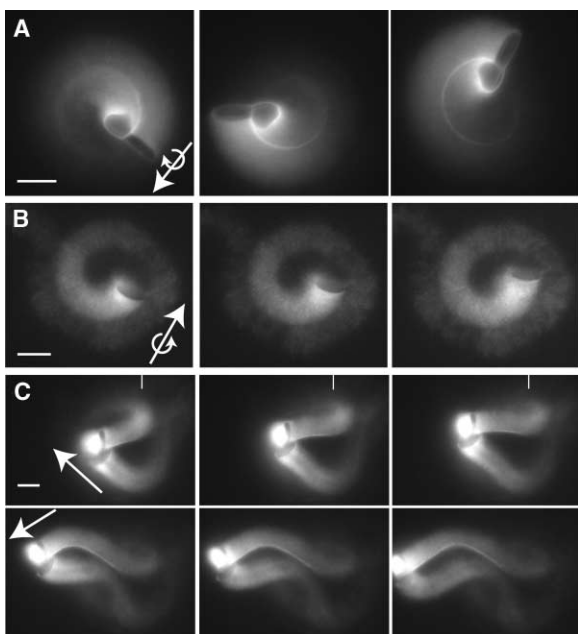


Figure 3. Motions Indicating Pushing on Flat Surfaces

(A) Circular motion of a disk-particle assembly. These frames from Movie 2 are 30 min apart. The particle is partially compressed. Inset shows the resultant clockwise moment and force that must exist to account for the motion.

(B) Spiraling disk with a single-face tail. These frames from Movie 3 are 10 min apart. Inset shows the resultant counterclockwise moment and force that must exist to account for the disk motion.

(C) Translational motions of a two-disk assembly. The sequences shown in the top and bottom rows are separate episodes of translation along a normal to one of the disks. In the top sequence, a bright spot in the upper tail clearly moves backward in the image (compare to white line) despite the forward motion of the assembly. The time interval in each sequence (from Movie 4) is 4 min. The scale bar in (C) represents 3.5 μm . All other scale bars represent 5 μm .

both initiating and sustaining actin-based motility [2, 3, 10]. In initiating motility (symmetry breaking), elastic propulsion illustrates how circumferential or “hoop” stresses build as assembled networks are displaced by new polymerization at the curved surfaces of spherical particles or *Listeria* [2, 3]. Stresses build until a critical hoop stress is reached and a local fracture occurs [10]. The fracture allows gel stresses to relax as the particle is squeezed out of a symmetrical actin cloud. Supporting these ideas are data showing that spherical particles of smaller diameter (higher curvature) break symmetry faster than larger spheres [10], presumably because they achieve critical stresses more quickly. By these arguments, when gels are grown on particles with both curved and flat surfaces, they should fracture on curved surfaces and relax to flat surfaces to minimize stresses. Such a mechanism could explain why tails are typically positioned on the flat faces of disks. However, when we examine the position of tails on perimeters with mixed curvatures, we instead find that tail location is independent of local curvature (Figure 4).

Elastic propulsion theory also explains how a process of stress build-up, squeezing, slipping/relaxation can continue after symmetry breaking to give sustained mo-

tility [2]. A periodic or “hopping” motion has been documented in reconstitution studies and is thought to be a visible manifestation of this cycle [10]. Additionally, lipid vesicles moving by actin-based motion are deformed in a manner that implies squeezing [11, 12]. To date all examples of reconstituted motility have occurred on the curved surfaces of *Listeria* [13], spherical particles [8–10], or lipid vesicles [11, 12], raising the prospect that curvature-derived forces may be essential for actin-based pushing.

Here, we address the potential requirement of surface curvature by identifying specific examples of motility that strongly suggest pushing forces normal to flat surfaces (Figure 3). Because individual particles (at their perimeters) or particle aggregates do have regions that are not flat, we cannot be sure that curvature-derived hoop stresses do not exist in these examples, only that they are an unlikely explanation for the motions shown. Indeed, in our examples (Figures 3A and 3B) where particle rotation identifies pushing forces on flat faces, a curved surface replete with actin is found closest to the particle’s center of rotation, suggesting some resistive forces may occur there. Similarly in experiments with deforming vesicles, actin intensity is brightest at the regions of high curvature, which are presumably being dragged by associations with the tail [11, 12]. Thus hoop stresses, with their accompanying frictional tractions, may be responsible for allowing actin tails to hold onto convex shapes, but our examples suggest that other mechanisms exist to account for pushing on flat faces.

By examining the behavior of VCA-coated spheres with different diameters, Bernheim-Groswasser et al. [10] provide several lines of evidence suggesting curvature-dependent forces. Our experiments with disks represent the limit of no curvature and give some apparently contradictory findings. First, Bernheim-Groswasser et al. report that VCA-coated spheres move more slowly at lower curvatures (larger diameters) [10], while we find that disks move faster than the spheres they are manufactured from. Bernheim-Groswasser et al. also find that hopping is more pronounced on larger (curvature $<0.25 \mu\text{m}^{-1}$) VCA-saturated spheres. We find that disks pushed on their large, flat surfaces do not hop, while disks moving via perimeter tails occasionally do. These discrepancies may be partly due to differences in ActA versus VCA-based motility and the use of extracts versus pure proteins, but they may also indicate that factors other than curvature are important for determining particle speeds and for triggering the hopping phenomenon. Others have shown that a wide range of ActA surface density appears to have minor effects on particle speeds in extracts [8, 14], but other physical parameters such as the particle’s surface area, the tail’s size or density, and the nature of the interactions of the particle with the walls of the motility chamber may all be important influences.

To be clear, elasticity theories do not preclude pushing against a flat surface, but they offer no mechanism for pushing in this limit. Only in the presence of curvature do the existing theories explain that antagonistic stresses will build across the dimensions of the gel to give motion (elastic propulsion). Elastic, antagonistic stresses also occur in molecular ratchet theories [4, 5],

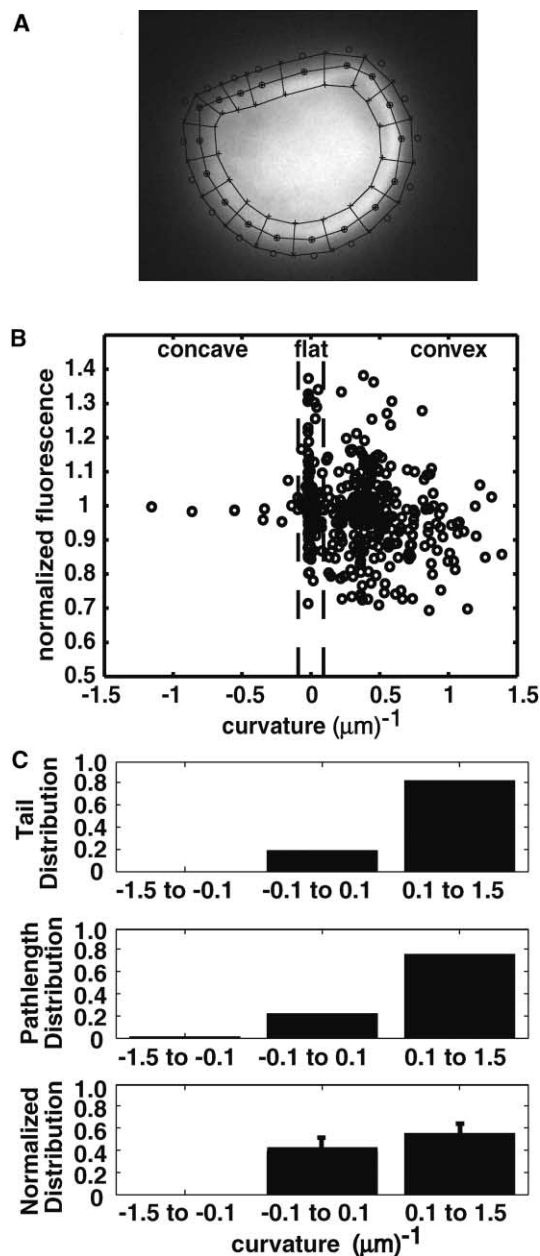


Figure 4. Curvature Effects on Cloud Nucleation and Tail Formation (A) Digitizing disk perimeters. Approximately 20 points/particle defined the perimeter of a disk. Local curvature and regions of interest (ROIs) were constructed from the digitized curves (see Supplemental Experimental Procedures). ROIs were used to integrate the local fluorescence or to detect tails and correlate them with local curvature.

(B) Correlation of perimeter fluorescence with curvature. Curvature was defined as concave: -1.5 to $-0.1 \mu\text{m}^{-1}$, flat -0.1 to $0.1 \mu\text{m}^{-1}$, or convex 0.1 to $1.5 \mu\text{m}^{-1}$ on 413 points from 18 microdisks. Fluorescence values are normalized to the mean fluorescence for each disk and show no correlation with curvature (cross correlation coefficient = 0.05).

(C) Correlation of tail appearances with local curvature. Histograms show raw appearances of tails on perimeters (top), the distribution of curvature along the particle perimeters (middle) and tail appearances normalized to curvature distributions (bottom). 53 tails were identified on 51 disks with mixed curvature perimeters between 3 and 5 hr after introducing particles into extracts. A bootstrap

but these are on a molecular scale and carried by the filaments touching the motile surface. One unifying idea is that molecular ratchets may provide the molecular origins of gel stresses for elastic propulsion at high curvature. However, ratchet theories are also compatible with the assumption that leading filaments are anchored to a perfectly rigid tail [4, 5], and ratchets need not be the molecular origins for stresses in elastic propulsion. Thus while elastic propulsion and molecular ratchets are compatible, they are also distinguishable and must be tested separately. Our work with motile disks does not challenge the existence of elastic propulsion. It does support the existence of molecular ratchets, but only because they provide viable mechanisms for pushing on a flat surface. Identifying such mechanisms is important because a network advancing a lamellipodium is pushing against a concave (or locally flat) front. If actin-based pushing in reconstituted systems resembles that at the leading edge of cells, then the common mechanism should not require substrate curvature.

Supplemental Data

Supplemental materials contain additional methodological detail, tabulated data on the evolution of disk configurations, movie versions of the time-lapse sequences in Figures 2C and 3 (Movies 1–4), two movies of disks pushed by perimeter tails (Movies 5 and 6), and one supplemental figure. The Supplemental Data is available at <http://www.current-biology.com/cgi/content/full/14/12/1094/DC1>.

Acknowledgments

The authors thank Schwartz's Forge and Metalworks, Inc. (Deansboro, NY) for help building the custom screw press and Brian McIntyre for help with electron microscopy. We thank Daniel Portnoy (University of California, Berkeley) for *L. monocytogenes* strain DPL4010, and Lisa Cameron (University of North Carolina, Chapel Hill), and Cyrus Wilson and Julie Theriot (Stanford University) for assistance with ActA purification. Thanks to Lisa Cameron, Soichiro Yamada, and Jamie Roussie for helpful comments on the text. This work was supported by University of Rochester start-up monies.

Received: January 3, 2004

Revised: April 13, 2004

Accepted: April 26, 2004

Published: June 22, 2004

References

1. Forscher, P., and Smith, S.J. (1988). Actions of cytochalasins on the organization of actin filaments and microtubules in a neuronal growth cone. *J. Cell Biol.* 107, 1505–1516.
2. Gerbal, F., Chaikin, P., Rabin, Y., and Prost, J. (2000). An elastic analysis of *Listeria monocytogenes* propulsion. *Biophys. J.* 79, 2259–2275.
3. Noireaux, V., Golsteyn, R.M., Friederich, E., Prost, J., Antony, C., Louvard, D., and Sykes, C. (2000). Growing an actin gel on spherical surfaces. *Biophys. J.* 78, 1643–1654.
4. Dickinson, R.B., and Purich, D.L. (2002). Clamped-filament elongation model for actin-based motors. *Biophys. J.* 82, 605–617.
5. Mogilner, A., and Oster, G. (2003). Force generation by Actin polymerization II: the elastic ratchet and tethered filaments. *Biophys. J.* 84, 1591–1605.
6. Tilney, L., and Portnoy, D. (1989). Actin filaments and the growth,

analysis (see Supplemental Experimental Procedures) indicates that the normalized appearances are not statistically different between curved and flat regions. Error bars represent the standard deviations from the bootstrap analysis.

movement and spread of the intracellular bacterial parasite *Listeria monocytogenes*. *J. Cell Biol.* **109**, 1597–1608.

7. Kocks, C., and Cossart, P. (1993). Directional actin assembly by *Listeria monocytogenes* at the site of polar surface expression of the actA gene product involving the actin-bundling protein plastin (fimbrin). *Infect. Agents Dis.* **2**, 207–209.
8. Cameron, L.A., Footer, M.J., van Oudenaarden, A., and Theriot, J.A. (1999). Motility of ActA protein-coated microspheres driven by actin polymerization. *Proc. Natl. Acad. Sci. USA* **96**, 4908–4913.
9. Wiesner, S., Helfer, E., Didry, D., Ducouret, G., Lafuma, F., Carlier, M.F., and Pantaloni, D. (2003). A biomimetic motility assay provides insight into the mechanism of actin-based motility. *J. Cell Biol.* **160**, 387–398.
10. Bernheim-Groswasser, A., Wiesner, S., Golsteyn, R.M., Carlier, M.F., and Sykes, C. (2002). The dynamics of actin-based motility depend on surface parameters. *Nature* **417**, 308–311.
11. Upadhyaya, A., Chabot, J.R., Andreeva, A., Samadani, A., and Van Oudenaarden, A. (2003). Probing polymerization forces by using actin-propelled lipid vesicles. *Proc. Natl. Acad. Sci. USA* **100**, 4521–4526.
12. Giardini, P.A., Fletcher, D.A., and Theriot, J.A. (2003). Compression forces generated by actin comet tails on lipid vesicles. *Proc. Natl. Acad. Sci. USA* **100**, 6493–6498.
13. Theriot, J.A., Rosenblatt, J., Portnoy, D.A., Goldschmidt-Clermont, P.J., and Mitchison, T.J. (1994). Involvement of profilin in the actin-based motility of *L. monocytogenes* in cells and in cell-free extracts. *Cell* **76**, 505–517.
14. Cameron, L.A., Svitkina, T.M., Vignjevic, D., Theriot, J.A., and Borisy, G.G. (2001). Dendritic organization of actin comet tails. *Curr. Biol.* **11**, 130–135.